Heme oxygenase-1 protects airway epithelium against apoptosis by targeting the proinflammatory NLRP3–RXR axis in asthma

Received for publication, July 26, 2018, and in revised form, September 5, 2018 Published, Papers in Press, October 17, 2018, DOI 10.1074/jbc.RA118.004950

Jiajia Lv[‡1], **Wen Su**[‡1], **Qianying Yu**[‡], **Meng Zhang**[‡], **Caixia Di**[‡], **Xiaoliang Lin**[‡], **Min Wu**[§2], and **Zhenwei Xia**[‡3]

From the [‡]*Department of Pediatrics and Department of Pulmonary & Critical Care Medicine, Ruijin Hospital, Shanghai Jiao Tong University School of Medicine, Shanghai 200025, China and the* [§]*School of Medicine & Health Sciences, Department of Biomedical Sciences, University of North Dakota, Grand Forks, North Dakota 58202*

Edited by Xiao-Fan Wang

Asthma is thought to be caused by malfunction of type 2 T helper cell (Th2)–mediated immunity, causing excessive inflammation, mucus overproduction, and apoptosis of airway epithelial cells. Heme oxygenase-1 (HO-1) functions in heme catabolism and is both cytoprotective and anti-inflammatory. We hypothesized that this dual function may be related to asthma's etiology. Using primary airway epithelial cells (pAECs) and an asthma mouse model, we demonstrate that severe lung inflammation is associated with rapid pAEC apoptosis. Surprisingly, NOD-like receptor protein 3 (NLRP3) inhibition, retinoid X receptor (RXR) deficiency, and HO-1 induction were associated with abrogated apoptosis. MCC950, a selective small-molecule inhibitor of canonical and noncanonical NLRP3 activation, reduced RXR expression, leading to decreased pAEC apoptosis that was reversed by the RXR agonist adapalene. Of note, HO-1 induction in a mouse model of ovalbumin-induced eosinophilic asthma suppressed Th2 responses and reduced apoptosis of pulmonary pAECs. *In vitro*, HO-1 induction desensitized cultured pAECs to ovalbumin-induced apoptosis, confirming the *in vivo* observations. Critically, the HO-1 products carbon monoxide and bilirubin suppressed the NLRP3–RXR axis in pAECs. Furthermore, HO-1 impaired production of NLRP3–RXR–induced cytokines (interleukin [IL]-25, IL-33, thymic stromal lymphopoietin, and granulocyte-macrophage colony-stimulating factor) in pAECs and lungs. Finally, we demonstrate that HO-1 binds to the NACHT domain of NLRP3 and the RXRα and RXRβ subunits and that this binding is not reversed by Sn-protoporphyrin. Our findings indicate that HO-1 and its products are essential for pAEC survival to maintain airway epithelium homeostasis during NLRP3–RXR–mediated apoptosis and inflammation.

Allergic asthma is characterized by chronic airway inflammation largely triggered by Th2 responses, which is initiated by both airway epithelial cells and antigen-presenting cells, such as dendritic cells (DCs)[4] and basophils (1). Allergen challenge results in airway epithelial inflammation and dysfunction. Under such a condition, airway epithelial cells undergo apoptosis. Two pathways basically categorize the sequence of events that culminate in the activation of aspartase-specific cysteine proteases, caspases: the extrinsic and the intrinsic pathways (2). The extrinsic pathway can be initiated by one of several cell surface death receptors (tumor necrosis factor receptor 1 and Fas receptor) when bound by the appropriate ligand. The intrinsic pathway is characterized by the permeabilization of the outer mitochondrial membrane and the release of several pro-apoptotic factors, including cytochrome *c*, into the cytosol. These factors are regulated by the Bcl-2 family including Bcl-2 and Bcl-XL (3–5). Physiologically, apoptotic epithelial cells are cleared via engulfment by phagocytes to maintain homeostasis (2). However, in asthma, this dynamic balance is disturbed because aberrant airway epithelial apoptosis may overwhelm the engulfment ability of the phagocytes. Defective or delayed engulfment of apoptotic cells in the lung of ovalbumin (OVA)-challenged mice showed exacerbated airway inflammation with elevated Th2 cytokines and airway hyper-responsiveness compared with mice with effective treatment of apoptotic cells (6). Previous studies have shown that epithelial damage and shedding are cardinal features of airway remodeling in patients with asthma and correlates with disease severity (7, 8). It was also reported that ciliated epithelial cells from patients with severe asthma exhibited increased apoptosis because of decreased cleavage of Fas ligand by Th2 cytokine exposure (8). Another study showed a p52-dependent epithelial apoptosis, but p52 overexpression alone did not induce significant inflammation (9). Thus, the mechanisms by which mediate airway epithelial cell apoptosis are largely uncharacterized. Studying how airway

This work was supported by National Natural Science Foundation of China Grants 91542202, 81470217, and 81200016 and by National Institutes of Health Grant R01 AI109317-01A1. The authors declare that they have no conflicts of interest with the contents of this article. The content is solely the responsibility of the authors and does not necessarily represent the official views of the National Institutes of Health.

[1] These authors contributed equally to this work.
[2] To whom correspondence may be addressed. E-mail: min.wu@med.und.edu.
[3] To whom correspondence may be addressed. Tel.: 86-21-64370045; Fax: 86-21-64333548; E-mail: xzw10484@rjh.com.cn.

[4] The abbreviations used are: DC, dendritic cell; BALF, bronchoalveolar lavage fluid; CCL2, C–C chemokine ligand-2; GM-CSF, granulocyte-macrophage colony-stimulating factor; HO-1, heme oxygenase-1; NLRP3, NOD-like receptor protein 3; OVA, ovalbumin; pAEC, primary airway epithelial cell; RXR, retinoid X receptor; TSLP, thymic stromal lymphopoietin; SnPP, Sn-protoporphyrin IX; IL, interleukin; TUNEL, terminal deoxynucleotidyl transferase–mediated dUTP nick end labeling; IP, immunoprecipitation; FBS, fetal bovine serum.

inflammation affects airway epithelial apoptosis and which mechanism modulates this process may provide insight into signaling pathways and indicating therapeutic targets to control inflammation.

Airway epithelial inflammation occurs in part in response to NACHT domain–, leucine-rich repeat–, and PYD-containing protein 3 (NLRP3) activation as well as the pro-inflammatory milieu in the lung (10). NLRP3 functions as a pathogen recognition receptor to recognize pathogen-associated molecular patterns (11). NLRP3 belongs to the NOD-like receptor subfamily of pathogen recognition receptors and along with the adaptor ASC protein PYCARD forms a caspase-1–activating complex known as the NLRP3 inflammasome. Upon danger signal stimulation, ASC protein and caspase-1 are recruited to the inflammasome complex. Within the activated NLRP3 inflammasome complex, caspase-1 activates the inflammatory cytokine, IL-1β (12). It has been reported that NLRP3, caspase-1, and IL-1β all contribute to the production of type 2 cytokines and pathogenesis of asthma (13–15). In addition, NLRP3 contributes to target-organ damage in type 2 diabetes and cardiovascular and renal diseases (16, 17). However, it is unknown whether NLRP3 modulates airway epithelial cell apoptosis to control allergic lung inflammation.

Nuclear receptors as superfamily members of transcriptional regulators play critical roles as signal transducers in immune functions. Within the nuclear receptors, the retinoid X receptor isotypes (RXR$\alpha/\beta/\gamma$) play a key role as heterodimeric partners for some nuclear receptors and are critical for Th2-mediated immunity. Blockade of RXR by an antagonist inhibited Th2 differentiation, resulting in reduced production of IL-4, IL-10, and IL-13 (18–20). Ligands for RXR$\alpha/\beta/\gamma$ show promise as therapeutic agents for allergic diseases, such as acne (21). RXR$\alpha/\beta/\gamma$ is activated by 9-*cis*-retinioc acid, a metabolite of vitamin A. Activation of RXR$\alpha/\beta/\gamma$ has been shown to inhibit Th1 response and to promote Th2 differentiation (18). In addition, RXR$\alpha/\beta/\gamma$ participates in the induction of cell apoptosis. It has been reported that RXR$\alpha/\beta/\gamma$ agonist (retinoic acid) induces apoptosis of tumor cells by activation of both inducible and endothelial nitric-oxide synthase and production of apoptogenic NO (22, 23). Because RXR alone and in combination with other nuclear hormone receptors also promotes Th2 differentiation (18), we wondered whether RXR could be exploited to block airway epithelium apoptosis in asthma.

Heme oxygenase-1 (HO-1), a member of the protein family of heat shock proteins, exerts both airway epithelial-protective and anti-inflammatory function. Most physiological functions of HO-1 have been associated with its enzymatic activity in heme catabolism, displaying an indispensable role in multiple inflammatory diseases by its anti-oxidant and anti-inflammatory properties (24). HO-1 can be induced by a variety of stimulus such as heat shock, cytokines, nitric oxide, endotoxin and hyperoxia, all of which are produced in asthma. It was reported that mice lacking HO-1 develop severe inflammatory disease (25). The protective role of HO-1 has been found in a variety of inflammatory models (26–28). We and others have previously demonstrated that pharmacological induction of HO-1 alleviates allergic airway inflammation in the lung and other organs, in which HO-1 dampens Th2 and Th17 cell differentiation (29–31). However, whether HO-1 suppresses airway epithelial apoptosis and inflammatory response through NLRP3 or RXR$\alpha/\beta/\gamma$ is unclear. Here, we demonstrated that activation of NLRP3–RXR$\alpha/\beta/\gamma$ axis promotes airway epithelial apoptosis and aggravates type 2 immune responses, whereas HO-1 efficiently inhibits this pathway and subsequent events in OVA-induced murine model of asthma.

Results

NLRP3 participates in OVA-induced allergic airway inflammation and airway epithelial cell apoptosis

To determine the functional role of NLRP3 in allergic airway inflammation, we established an OVA-induced mice model of eosinophilic asthma and administrated with or without MCC950, a small-molecule inhibitor of NLRP3. We showed that OVA stimulation led to a significant increase in basophils but not DCs infiltration into the lung, which was blunted by MCC950 (Fig. 1*A*). In addition, MCC950 pretreatment severely reduced pulmonary thymic stromal lymphopoietin (TSLP) and C–C chemokine ligand-2 (CCL2) compared with OVA-induced mice (Fig. 1*B*). As expected, inhibition of NLRP3 significantly suppressed the release of IL-1β, which is produced after catalysis of pro-IL-1β by NLRP3 (Fig. 1*B*). Importantly, NLRP3 inhibition resulted in robust decrease in type 2 cytokines (IL-4, IL-5, and IL-13), serum OVA-specific IgE (OVA-sIgE) (Fig. 1*C*), mucus secretion, and inflammatory cell infiltration (Fig. 1*D*). These data demonstrate that NLRP3 is required for OVA-induced allergic responses.

It is generally accepted that NLRP3 activation induced by ROS generation in pathogenic or injury conditions mediates allergic Th2 responses. Excessive oxidant products and Th2 cytokines produce a milieu that damages the airway epithelial cells and promotes apoptosis. Apoptosis is a key component of normal cellular homeostasis, whereas dysregulation of this process aggravates airway inflammation (32, 33). Therefore, we investigated the effect of NLRP3 on airway epithelial apoptosis by TUNEL assay and revealed an increase in airway epithelial cells in OVA-induced asthmatic mice. This was dramatically decreased by MCC950, consistent with the ratio of TUNEL-positive airway epithelial cells and paralleled to Th2 responses (Fig. 1*E*). Thus, TUNEL positivity reflected the extent of inflammation and was associated with resolution of airway inflammation.

NLRP3–RXR$\alpha/\beta/\gamma$ axis drives bronchial epithelial cell apoptosis and inflammatory cytokine production

To further verify that NLRP3 expression is related to the apoptosis of airway epithelial cells, we determined the level of Bcl-XL, an anti-apoptotic protein, in primary airway epithelial cells (pAECs) pretreated with or without MCC950. The results showed that OVA-induced NLRP3 significantly suppressed Bcl-XL expression, which was reversed by MCC950, indicating a decrease in apoptosis of pAECs (Fig. 2*A*). Because RXR$\alpha/\beta/\gamma$ is a promising regulator of apoptotic pathways in various cell types, we next investigated whether RXR$\alpha/\beta/\gamma$ regulates pAECs apoptosis. Adapalene, a robust RXR$\alpha/\beta/\gamma$ agonist, was used subsequently. Compared with the OVA-stimulated group, adapalene addition led to a further decrease in Bcl-XL (Fig. 2*B*).

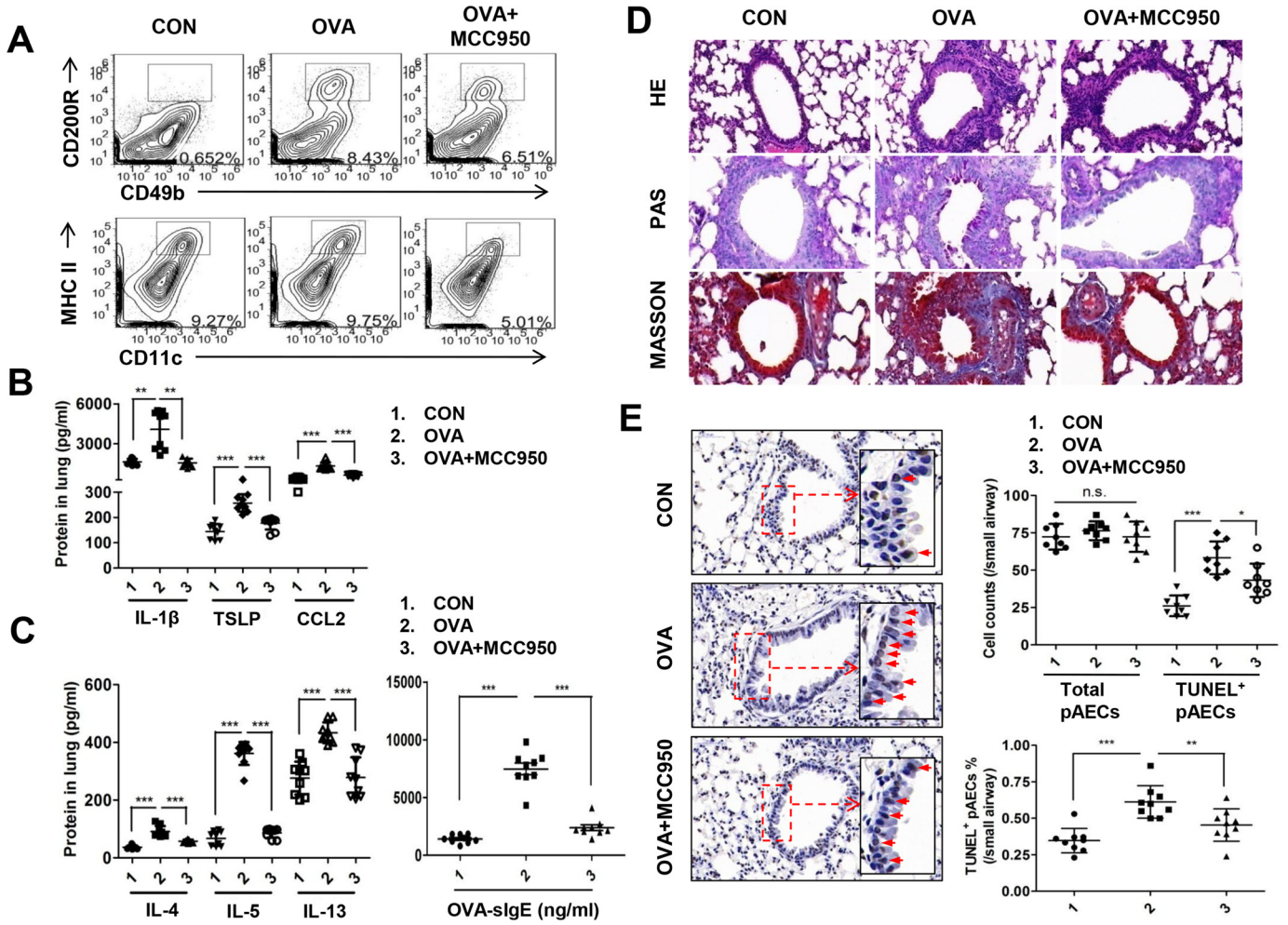

Figure 1. NLRP3 participates in OVA-induced allergic airway inflammation and airway epithelial cell apoptosis. OVA-sensitized and challenged mice (OVA group) were injected intraperitoneally with MCC950 (OVA + MCC950 group). The mice received normal saline with $Al(OH)_3$) intraperitoneally on days 0 and 14 and normal saline on days 14, 25, 26, and 27 were set as the control group (*CON*). *A*, flow cytometry analysis of DCs and basophils in lungs. *B*, the levels of TSLP, CCL2, and IL-1β in lung homogenates. *C*, the levels of IL-4, IL-5, and IL-13 in lung and OVA-sIgE in serum. *D*, representative images of proximal airways showing inflamed lung areas, mucus-producing cells per epithelium length, airway collagen content, and smooth muscle thickness. *E*, TUNEL assay of apoptotic cells of airways in lung tissues. For analysis of flow cytometry, ELISA, and TUNEL assay, data were pooled from three independent experiments with three mice each. One representative flow analysis for basophils and DCs, one representative lung histology, or one representative TUNEL assay of three independent experiments with three mice each is shown. The data are shown as means ± S.D. *, $p < 0.05$; **, $p < 0.01$; ***, $p < 0.001$.

We next explored whether RXR$\alpha/\beta/\gamma$ is involved in NLRP3-induced apoptosis in airway epithelial cells and found that the expression of RXR$\alpha/\beta/\gamma$ was significantly reduced in pAECs treated with MCC950 (Fig. 2*C*). Similarly, the early and advanced apoptosis of pAECs after MCC950 treatment was decreased compared with the OVA-stimulated group (Fig. 2*D*). However, decreased apoptosis after NLRP3 inhibition by MCC950 was reversed after activation of RXR by adapalene (Fig. 2*D*). These results indicate that NLRP3 expression activates RXR$\alpha/\beta/\gamma$ and that NLRP3–RXR$\alpha/\beta/\gamma$ axis participates in the induction of bronchial epithelial cell apoptosis.

We then evaluated changes in epithelial cell-derived pro-allergic cytokine production and observed significant decreases in IL-25, IL-33, TSLP, and granulocyte-macrophage colony stimulating factor (GM-CSF) by MCC950 treatment but robust increases by adapalene (Fig. 2*E*). These data indicate that NLRP3–RXR$\alpha/\beta/\gamma$ axis directs production of inflammatory cytokines from airway epithelial cells.

HO-1 induction alleviates allergic airway inflammation

Our previous studies showed that HO-1 exhibits protective roles in airway inflammation (34). Thus, we evaluated the levels of cytokines and inflammatory cell infiltration in the lungs of asthmatic murine model. We detected IL-1β and found that HO-1 induction *in vivo* with hemin effectively reduced the level of IL-1β in the lung (Fig. 3*A*) along with a decrease in TSLP and CCL2 (Fig. 3*B*). Eosinophil recruitment in bronchoalveolar lavage fluid (BALF) in the lung was markedly inhibited in the OVA + hemin group compared with that in OVA-challenged group (Fig. 3*C*). In addition, Th2 cytokines including IL-4, IL-5, and IL-13 in lungs and OVA–sIgE in serum were dramatically reduced in OVA + hemin group mice (Fig. 3*D*). Lastly, the recruitment of peribronchial eosinophils and lymphocytes, together with mucus hypersecretion, was dramatically alleviated in lungs in OVA + hemin group mice compared with those in OVA-challenged mice (Fig. 3*E*). Collectively, these results demonstrate that HO-1 can suppress airway inflammation in this murine model.

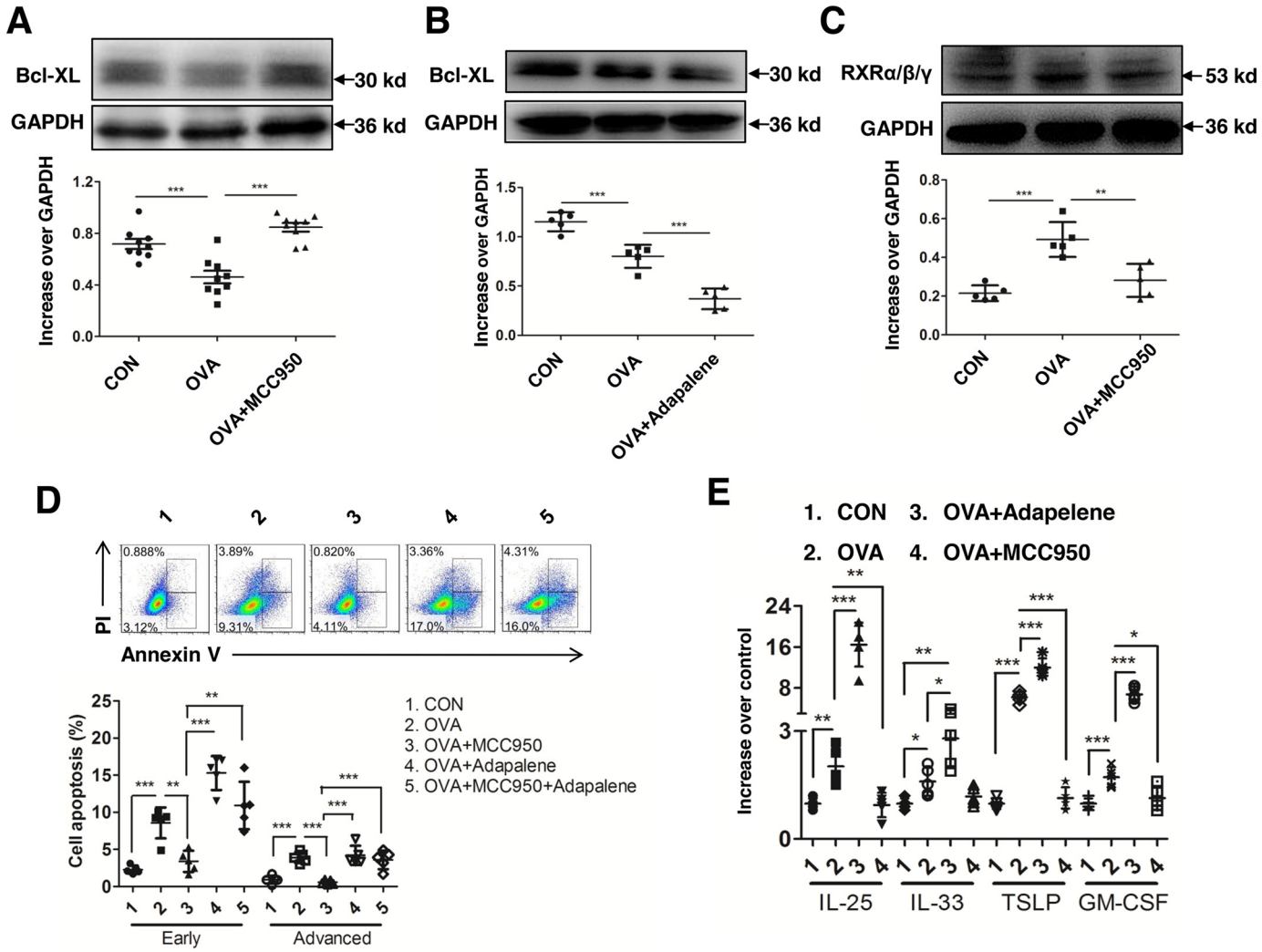

Figure 2. NLRP3–RXRα/β/γ axis drives bronchial epithelial cell apoptosis and inflammatory cytokines production *in vitro*. pAECs were treated with MCC950 (OVA + MCC950 group) or adapalene (OVA + adapalene group) or MCC950 followed by adapalene (OVA + MCC950 + adapalene group) and were subsequently stimulated with OVA dissolved in PBS. PBS-treated pAECs were as control (*CON*). *A* and *B*, expression of Bcl-XL in pAECs after treatment with MCC950 (*A*) or adapalene (*B*). *C*, expression of RXRα/β/γ in pAECs after treatment with MCC950. *D*, flow cytometry analysis of OVA-induced early and advanced apoptosis in pAECs. *E*, expression of cytokines in OVA-induced pAECs treated with MCC950 and adapalene. For statistical analysis of Western blotting and flow cytometry, data are pooled from five independent experiments. One representative Western blotting and flow analysis of five independent experiments are shown. The data are shown as means ± S.D. *, $p < 0.05$; **, $p < 0.01$; ***, $p < 0.001$.

HO-1 induction inhibits NLRP3–RXRα/β/γ axis–mediated cell apoptosis in lungs

To gain insights into the biological relevance of HO-1–mediated anti-apoptosis in airway epithelial cells in *vivo*, we pretreated WT mice with hemin to induce HO-1 expression before OVA sensitization and subsequently challenged with OVA. We observed that hemin-induced HO-1 decreased the expression of RXRα/β/γ but increased expression of Bcl-XL in the lungs of WT mice. Expression of NLRP3 was not different between WT and hemin-treated mice (Fig. 4*A*). However, induction of HO-1 impaired expression of NLRP3 and RXRα/β/γ while significantly increasing the expression of Bcl-XL in lungs of OVA- and hemin-treated mice compared with that in OVA-induced mice (Fig. 4*B*), suggesting that HO-1 can inhibit cell apoptosis. TUNEL assay of lung histology showed that hemin treatment led to an obvious decrease in apoptotic airway epithelial cells (Fig. 4*C*). Manual counting showed that the number of total airway epithelial cells was not significantly different among four groups. However, the number of TUNEL-positive epithelial airway cells in OVA- and hemin-treated mice was dramatically decreased compared with that in OVA-challenged mice (Fig. 4*D*). The ratio of TUNEL-positive airway epithelial cells to total cells was also consistently decreased in OVA- and hemin-treated mice compared with that in OVA-challenged mice (Fig. 4*E*).

HO-1 dampens NLRP3–RXRα/β/γ axis to reduce apoptosis in pAECs

To gain a better understanding of the molecular mechanisms of HO-1, we used pAECs to examine whether hemin can induce expression of HO-1. The results showed that the expression of HO-1 was highly up-regulated in pAECs at 2 h after hemin treatment and increased in a hemin concentration-dependent manner (Fig. 5*A*). It has been reported that HO-1 exerts its anti-apoptotic function through its products, CO and bilirubin; thus, we used CO-releasing molecule (CO-RM2) and bilirubin

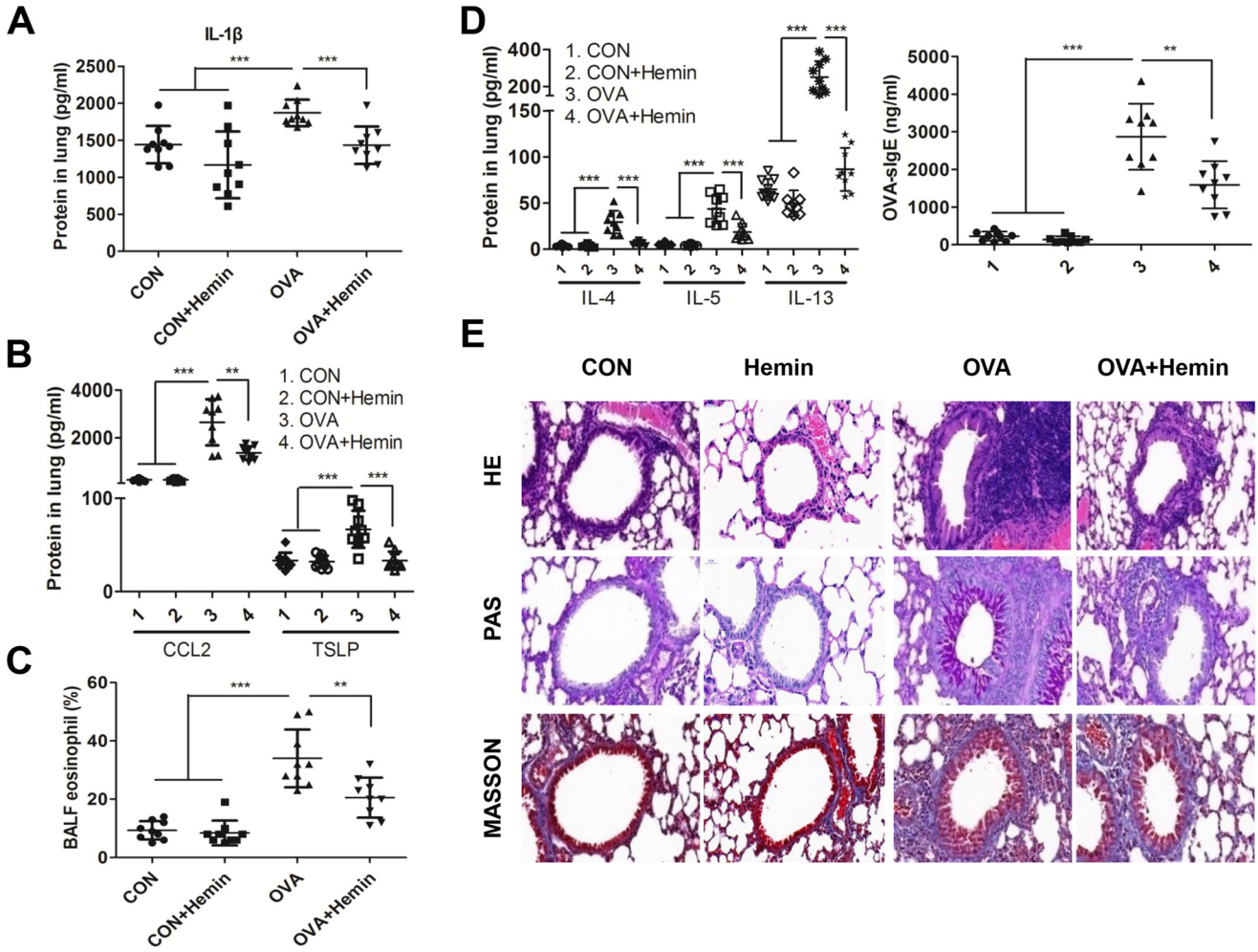

Figure 3. HO-1 induction mitigates allergic airway inflammation. OVA-sensitized and challenged mice (OVA group) were injected intraperitoneally with hemin (OVA + hemin group). A control group (*CON*) was set as described for Fig. 1. *A*, the level of IL-1β in lung homogenates. *B*, the levels of TSLP and CCL2 in lung homogenates. *C*, flow cytometry analysis of eosinophils in BALF. *D*, the levels of Th2 cytokines in lung homogenates and OVA–sIgE in serum. *E*, representative images of proximal airways showing inflamed lung areas, mucus-producing cells per epithelium length and airway collagen content, and smooth muscle thickness. For analysis of ELISA, data are pooled from three independent experiments with three mice each. One representative lung histology of three independent experiments with three mice each is shown. The data are shown as means ± S.D. **, $p < 0.01$; ***, $p < 0.001$.

to treat pAECs, respectively. The results demonstrated that pAECs treated with hemin, CO-RM2, or bilirubin decreased expression of NLRP3 and RXR but increased expression of Bcl-XL (Fig. 5*B*). We next determined whether HO-1 induction affects apoptosis of pAECs after stimulation with OVA or OVA + hemin, respectively. The results revealed that both early and late apoptosis of pAECs was rescued by hemin using flow cytometry analysis (Fig. 5*C*). In addition, we found that both CO-RM2 and bilirubin also reduced expression of NLRP3 and RXR$\alpha/\beta/\gamma$ and enhanced expression of Bcl-XL in OVA-stimulated pAECs (Fig. 5*D*). To further investigate the effect of HO-1 itself, Sn-protoporphyrin (SnPP), the HO-1 inhibitor, was used to suppress the enzymatic activity. The results showed that although changes in NLRP3, RXR$\alpha/\beta/\gamma$ and Bcl-XL expression was monitored; there was also decreased expression of NLRP3 and RXR$\alpha/\beta/\gamma$ but increased expression of Bcl-XL in the hemin + SnPP-treated group compared with the OVA and OVA + SnPP groups, having an effect similar to the hemin-, CO-RM2–, or bilirubin-treated groups (Fig. 5*D*). These results suggest that HO-1 itself can exert inhibitory effect on apoptosis of bronchial epithelial cells via the NLRP3–RXR$\alpha/\beta/\gamma$ axis.

In addition to an suppressive role in apoptosis, we observed that HO-1 decreased the IL-1β level in the supernatant of pAECs following OVA stimulation (Fig. 5*E*) and suppressed the expression of cytokines IL-25, IL-33, TSLP, and GM-CSF in airway epithelial cells (Fig. 5*F*). Thus, these results establish that HO-1 can suppress bronchial epithelial cell apoptosis and inflammation by dampening the NLRP3–RXR$\alpha/\beta/\gamma$ axis.

HO-1 binds to NACHT domain of NLRP3 and RXRα and RXRβ subunits in an enzymatic activity-independent manner to inhibit cell apoptosis

To characterize the interaction between HO-1 protein and NLRP3 or RXR$\alpha/\beta/\gamma$, we chose a human bronchial epithelial cell line (BEAS-2B) to obtain enough protein content to perform co-IP. Having treated BEAS-2B cells with hemin and OVA, we collected cell lysates and analyzed by Western blotting and co-IP, respectively. First, we found that hemin treatment decreased expression of NLRP3 and RXR$\alpha/\beta/\gamma$ and increased Bcl-XL in BEAS-2B cell (Fig. 6*A*), which is consistent with observations in pAECs. Next, using co-IP, we found that HO-1 bound to NLRP3 and RXR$\alpha/\beta/\gamma$ with or without SnPP

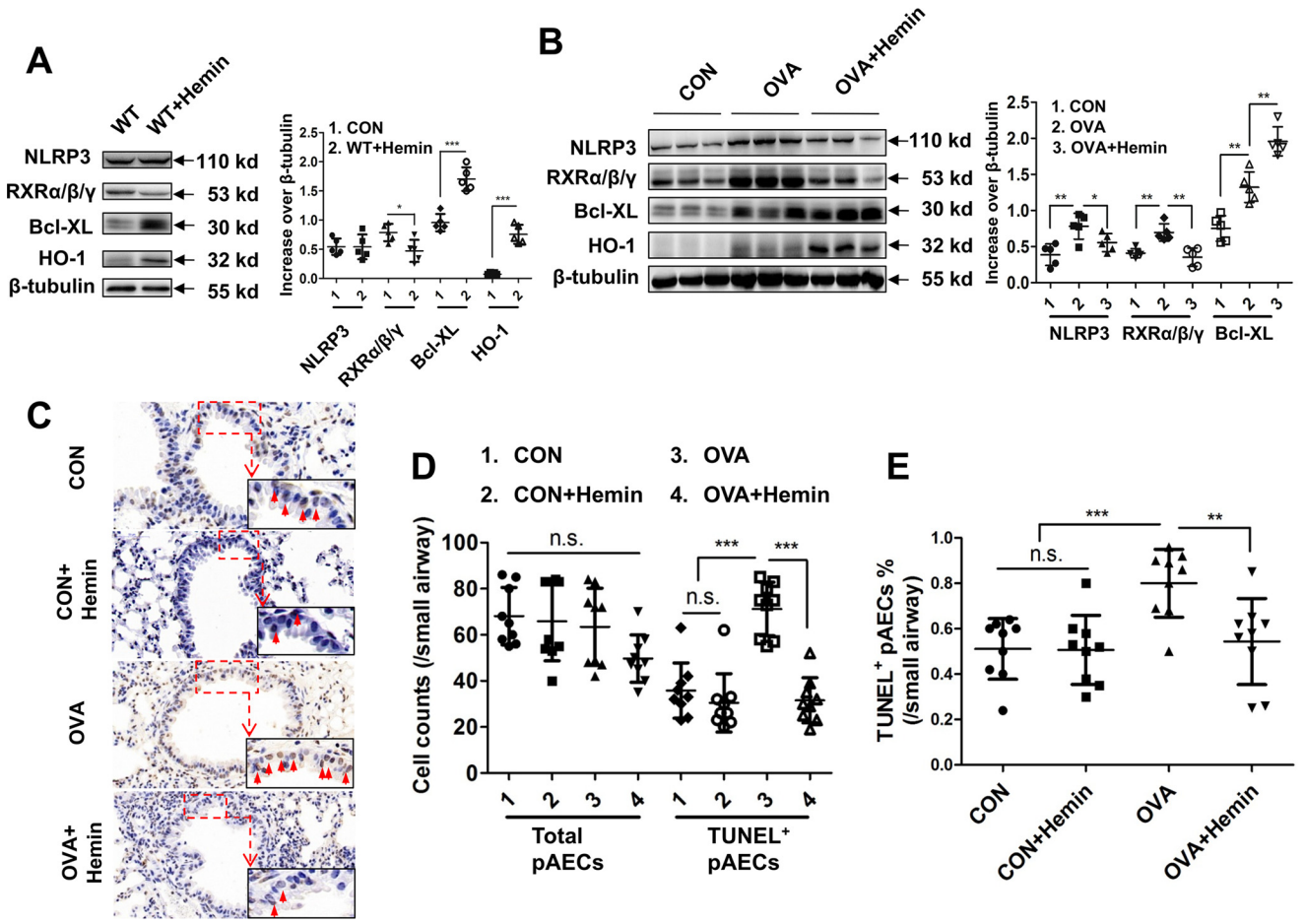

Figure 4. HO-1 induction inhibits NLRP3–RXR$\alpha/\beta/\gamma$ axis–mediated cell apoptosis in lungs. OVA-sensitized and challenged mice (OVA group) were injected intraperitoneally with hemin (OVA + hemin group). A control group (*CON*) was set as described for Fig. 1. *A*, expression of NLRP3, RXR$\alpha/\beta/\gamma$ and Bcl-XL in lung of WT mice after hemin treatment. *B*, expression of NLRP3, RXR$\alpha/\beta/\gamma$, and Bcl-XL in lung in OVA-induced murine model of asthma with or without hemin injection. *C*, TUNEL assay of lung sections. The *red arrows* indicate apoptotic airway epithelial cells. *D*, analysis of TUNEL-positive airway epithelial cells in the lung. Each value was obtained from at least three small airways per mouse. *E*, ratio of TUNEL-positive airway epithelial cells to total airway epithelial cells. For analysis of Western blotting and TUNEL assay, the data are pooled from three independent experiments with three mice each. One representative Western blotting and lung histology of three independent experiments with three mice each is shown. The data are shown as means ± S.D. *, $p < 0.05$; **, $p < 0.01$; ***, $p < 0.001$.

treatment (Fig. 6*B*), suggesting that the binding between HO-1 with NLRP3 or RXR$\alpha/\beta/\gamma$ is independent of HO-1 activity (Fig. 6*C*). Finally, to investigate which domain of NLRP3 and subunit of RXR$\alpha/\beta/\gamma$ interact with HO-1, four domains of NLRP3 (LRR, NACHT, Pyrin, and FISNA) or three subunits of RXR (RXRα, RXRβ, and RXRγ) and HO-1 expression plasmids were cotransfected into 293T cells, respectively. The results demonstrated that HO-1 mainly bound to NACHT domain of NLRP3 (Fig. 6*D*), as well as RXRα and RXRβ subunits (Fig. 6*E*), suggesting a potential role for HO-1 in regulating the biological function of NLRP3 and RXR$\alpha/\beta/\gamma$.

Studies showed that among three subunits of RXR$\alpha/\beta/\gamma$, RXRα interacts with DNA to regulate transcription of target genes in a ligand-dependent manner. In response to inflammation and apoptosis, it migrates from the nucleus to the cytoplasm and facilitates nuclear export of its heterodimerization partner Nur77 and anti-apoptotic protein Bcl-2 conversion, resulting in apoptosis (35–37). We further used siRNA to knock down RXRα expression and verify the effects of RXRα in pAECs apoptosis. We showed that suppression of RXRα significantly increased the expression of Bcl-XL (Fig. 6*F*), suggesting that RXRα participates in the modulation of pAECs apoptosis. Taken together, these data indicate that HO-1 exerts a crucial role in the anti-apoptotic response in airway epithelial cells through inhibiting RXRα.

Discussion

In this study, we find that HO-1 attenuates airway epithelial cell apoptosis and allergic airway inflammation. HO-1 represses the expression of NLRP3 and RXR in airway epithelial cells and thus inhibits apoptosis and inflammation. These findings enriched the current view of HO-1 function, providing better understanding of the role of epithelial apoptosis in allergic airway inflammation and opening the door for HO-1 as a new therapeutic target to control asthma and allergic diseases.

We employed a mouse model of OVA-induced allergic airway inflammation (38) by sensitization with OVA complexed with aluminum hydroxide ($Al(OH)_3$) and challenged mice with OVA in PBS. Adjuvant is reported to have a role in the development of Th2 response. In the current study, the role of adjuvant could be largely neglected between $Al(OH)_3$-sensitized and OVA-$Al(OH)_3$-sensitized mice because of both giving

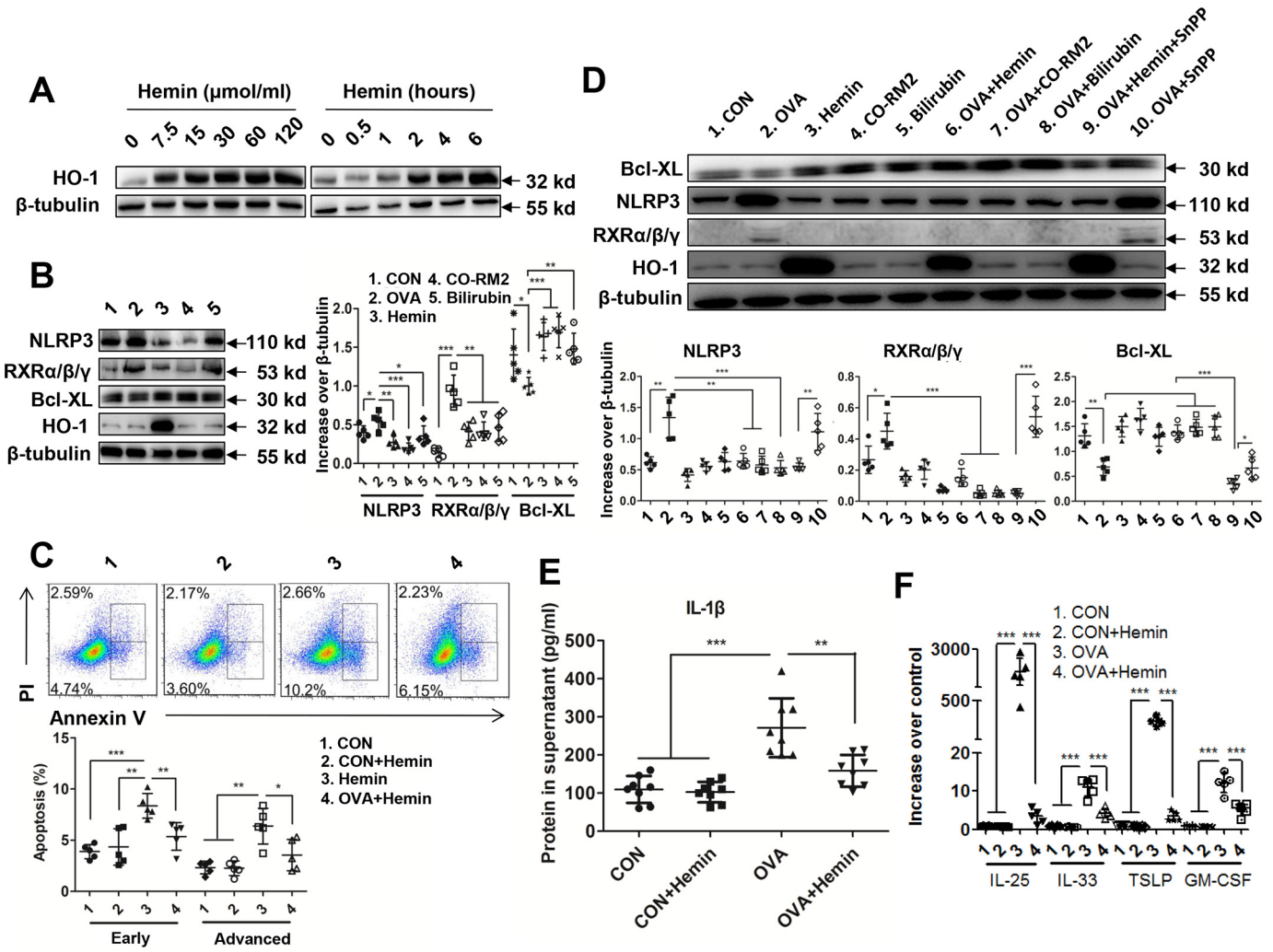

Figure 5. HO-1 dampens NLRP3–RXR$\alpha/\beta/\gamma$ axis to reduce apoptosis in pAECs. pAECs were stimulated with OVA, hemin, CO-RM2, and bilirubin or with OVA + hemin, OVA + CO-RM2, OVA + bilirubin, OVA + hemin + SnPP, and OVA + SnPP, respectively. A control group (*CON*) was set by treatment with PBS. *A*, HO-1 expression in pAECs. *B*, expression of NLRP3, RXR$\alpha/\beta/\gamma$, and Bcl-XL in pAECs with hemin, CO-RM2, and bilirubin treatment, respectively. *C*, flow cytometry analysis of apoptosis in pAECs with hemin treatment. *D*, expression of NLRP3, RXR$\alpha/\beta/\gamma$, and Bcl-XL in OVA-stimulated pAECs with treatment of hemin, CO-RM2, bilirubin, and SnPP. *E*, the level of IL-1β protein in the supernatant of pAECs cultures with hemin treatment. *F*, mRNA level of IL-25, IL-33, TSLP, and GM-CSF in OVA-stimulated pAECs with hemin treatment. For analysis of Western blotting, flow cytometry, and RT-PCR, data are pooled from five independent experiments. One representative Western blotting and flow cytometry of five independent experiments is shown. The data are shown as means ± S.D. *, $p < 0.05$; **, $p < 0.01$; ***, $p < 0.001$.

same dose of $Al(OH)_3$. By intersecting cell culture and animal data, we find a clear pro-apoptotic role of NLRP3. In the lung, NLRP3 expression was associated with increased apoptosis of airway epithelial cells. By employing MCC950, an NLRP3 inhibitor by blocking ASC oligomerization (39), we demonstrated that apoptosis of airway epithelial cells were markedly decreased by MCC950 pretreatment both *in vitro* and *in vivo*. This overall finding is in line with a previous study showing that in the context of diabetic nephropathy, NLRP3 inflammasome links cell apoptosis in the kidney (40). Importantly, we observed a positive regulatory effect of NLRP3 on RXR$\alpha/\beta/\gamma$, well known death molecules associated with proliferation and apoptosis in various cells. Previous studies also show that inhibition of RXR$\alpha/\beta/\gamma$ blocks Th2 cell differentiation and prevents allergic airway inflammation (20). Furthermore, using adapalene, an agonist of RXR$\alpha/\beta/\gamma$ that increases activity of caspase-3 and induces apoptosis via the Bax/Bcl-2 pathway (41), we found a pro-apoptotic effect of RXR$\alpha/\beta/\gamma$ in airway epithelial cells. These findings indicate a novel role for NLRP3–RXR$\alpha/\beta/\gamma$ axis in the regulation of airway epithelial homeostasis.

Induction of HO-1 by systemic hemin administration has been previously reported to alleviate Th2 and Th17 response in mice (31, 34). Indeed, much of our knowledge about HO-1 biology has relied on hemin, a promising compound in the induction of HO-1. Specifically, asthma is associated with increased risk of coagulation that can afflict or promote damage to red blood cells, ultimately leading to increased concentration of hemin *in vivo* (42). The degradation of hemin induces HO-1 synthesis with the release of CO, bilirubin, and iron (43). However, expression of HO-1 in the setting of allergic airway inflammation is not sufficient to exert anti-apoptosis and anti-inflammation. As seen in this study, the level of HO-1 in airway epithelial cells and lung of asthmatic mice showed slight but not significant increase, which is in line with our previous studies (31). Importantly, HO-1 is crucial for the clearance of hemin (44). In this study, we demonstrate that, upon OVA stimula-

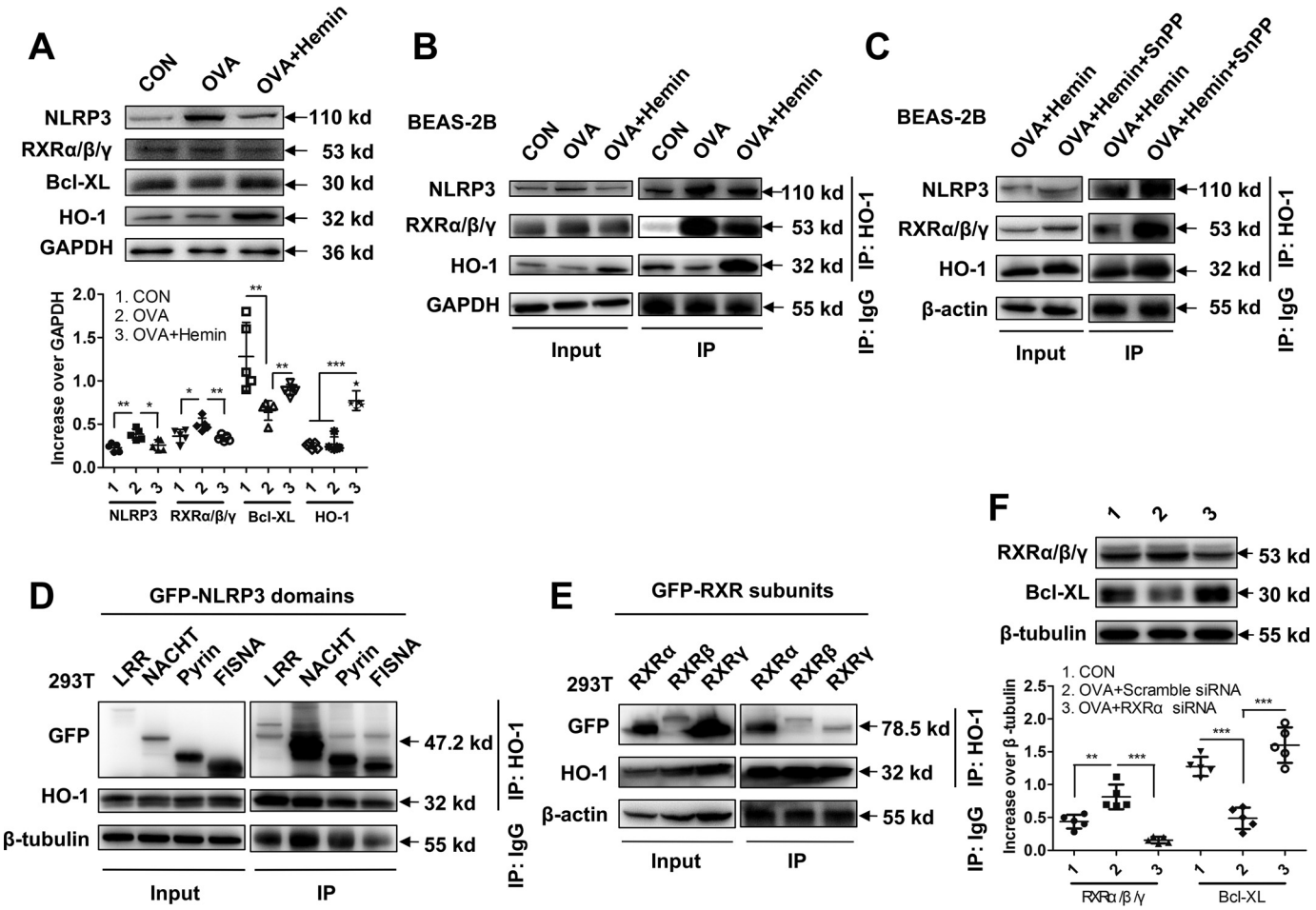

Figure 6. HO-1 bound to NACHT domain of NLRP3 and RXRα and RXRβ subunits in an enzymatic activity-independent manner to inhibit cell apoptosis. *A*, expression of NLRP3, RXR$\alpha/\beta/\gamma$, and Bcl-XL in BEAS-2B cells with hemin treatment. *B*, co-IP and Western blotting were used to observe HO-1 interaction with NLRP3 and with RXR$\alpha/\beta/\gamma$. The cells were stimulated with OVA (OVA group) or with OVA and hemin (OVA + hemin group). A control group was set by treatment with PBS (*CON*). GAPDH (36 kDa) was set as loading control in input. *C*, co-IP and Western blotting were used to observe HO-1 interaction with NLRP3 and RXR$\alpha/\beta/\gamma$ in the presence of SnPP. β-Actin (43 kDa) was set as a loading control in input. *D*, interaction between HO-1 and domains of NLRP3. The HO-1 and four GFP-labeled NLRP3 domain expression plasmids were co-transfected into 293T cells to identify the interaction sites of the NLRP3 domain with HO-1. β-Tubulin (55 kDa) was set as loading control in input. *E*, interaction between HO-1 and subunits of RXR$\alpha/\beta/\gamma$. The HO-1 and three GFP-labeled RXR$\alpha/\beta/\gamma$ subunit expression plasmids were co-transfected into 293T cells to identify the interaction sites of the RXR$\alpha/\beta/\gamma$ with HO-1. β-Actin (43 kDa) was set as loading control in input. *F*, expression of RXR$\alpha/\beta/\gamma$ and Bcl-XL in pAECs after treatment with RXRα siRNA. For analysis of Western blotting, data are pooled from five independent experiments. One representative Western blotting of five independent experiments is shown. The data are shown as means ± S.D. *, $p < 0.05$; **, $p < 0.01$; ***, $p < 0.001$.

tion, a higher frequency of apoptosis and lower expression of HO-1 in airway epithelial cells were induced. In contrast, increased HO-1 expression after hemin treatment was associated with decreased apoptosis of airway epithelial cells *in vitro* and *in vivo*. These results suggest a promising role for HO-1 in anti-apoptosis and anti-inflammation activities in airway epithelial cells and lung tissues.

It has been reported that HO-1, as well as its product CO, can inhibit NLRP3 inflammasome activation in lung injury and mastitis in mice (45, 46). In the context of allergic asthma, we found that HO-1, as well as its enzymatic products CO and bilirubin, negatively regulated NLRP3 expression and apoptosis of airway epithelial cells, consistent with an inhibitory role of HO-1 in apoptosis of other cell types (47, 48). We further observed that HO-1 directly bound to NLRP3, which is independent of HO-1 enzymatic activity after using SnPP and mainly bound to the NACHT domain of NLRP3. The NACHT domain is thought to function as an oligomerization domain, providing a scaffold where signal transduction complexes can be assembled (49, 50). Because binding of HO-1 may block signal transduction complex formation of NACHT domain, these results further support that HO-1 targets apoptosis-associated domain to play the inhibitory function. Notably, hemin-induced HO-1 and its products, CO and bilirubin, also rescued RXR$\alpha/\beta/\gamma$-mediated apoptosis of airway epithelial cells. These findings are consistent with a suppressive role of HO-1 in apoptosis as described in several previous studies (47, 48). We further demonstrated that HO-1 could bind RXR$\alpha/\beta/\gamma$ in an enzymatic activity-independent manner. Subunit specific analysis showed that the binding sites of HO-1 on RXR$\alpha/\beta/\gamma$ were RXRα and RXRβ. These results demonstrate for the first time that apoptosis of airway epithelial cells involves NLRP3–RXR$\alpha/\beta/\gamma$ axis and that HO-1 could regulate this process through binding NACHT domain and RXRα and RXRβ subunits, although interaction between HO-1 and RXRα is stronger. Because previous studies have shown that RXRα and RXRβ

may play distinct roles in gene regulation in other models (51, 52), it may be worth further studying whether RXRα and RXRβ have different roles in asthmatic conditions. Taking these results together, we envisage that anti-apoptotic function of HO-1 may depend on both HO-1 itself action and its enzymatic activity.

In addition to its anti-apoptotic role, HO-1 possesses strong anti-inflammatory properties by suppressing production of epithelial cell-derived cytokines induced by activation of NLRP3 inflammasome and RXR$\alpha/\beta/\gamma$. These findings are in agreement with previous studies showing the inhibitory role of HO-1 in apoptosis and inflammation and indicating that HO-1 may fine-tune pro- *versus* anti-inflammatory cell ratios, rendering significant predictive power in distinguishing pro- and anti-inflammatory conditions. In conclusion, we show a promising role for HO-1 in the reduction of airway epithelial cell apoptosis and alleviation of allergic lung inflammation. HO-1 may exert this anti-apoptotic and anti-inflammatory effect through suppression of the NLRP3–RXR$\alpha/\beta/\gamma$ axis.

Experimental procedures

Murine model of OVA-induced allergic airway inflammation

C57BL/6 WT mice were used and bred in our specific pathogen-free animal facility at Ruijin Hospital (Shanghai, China). The mice were maintained in a temperature-steady (23 °C) facility with access to food and water. All protocols were approved by the Ruijin Hospital animal research ethical committee and complied with the Chinese government's ethical and animal experiment regulations. To induce allergic airway inflammation, we employed a conventional OVA-induced asthmatic mouse model as previously described (38). Briefly, the mice were sensitized intraperitoneally with 0.2 ml (100 μg) of OVA (grade V; Sigma) complexed with aluminum hydroxide ($Al(OH)_3$) on days 0 and 14. On days 14, 25, 26, and 27, the mice were intranasally challenged with 0.5 mg of OVA in 50 μl of sterile PBS under light isoflurane anesthesia. The control group received normal saline with $Al(OH)_3$) intraperitoneally on days 0 and 14 and normal saline on days 14, 25, 26, and 27.

Administration of hemin or MCC95

WT or OVA-sensitized and challenged mice received an intraperitoneal injection of 75 μmol/kg in 200 μl of liquid hemin (Sigma–Aldrich) or 20 mg/kg in 200 μl of PBS MCC950 (Selleck) at days −2, −1, 12, 13, 23, and 24 as described before (29, 34, 53). In preparation of hemin for *in vivo* use, 12.5 g of hemin was dissolved in 0.1 mol/liter NaOH, diluted with PBS, and titrated to pH 7.5 with 0.2 mol/liter HCl. Control mice sensitized and challenged with OVA received 200 μl of normal PBS.

Tissue harvest and single-cell suspension preparation

24 h after the last OVA challenge, mice were sacrificed by CO_2 inhalation, and blood samples were collected for further OVA–sIgE analysis. The BALF was collected by injecting 0.4 ml of PBS (with 0.01 mmol/liter EDTA) and was centrifuged for cell collection. The inferior lobe of the right lung was fixed in 4% formaldehyde solution for histology analysis, and the other parts were minced, digested by collagenase IV (Sigma–Aldrich) in an incubator at 37 °C with 5% CO_2 for 30 min, and then passed through a 70-μm cell strainer for a single cell suspension. All experiments were performed three times using five animals of each group.

Primary airway epithelial cell isolation from mice

Tracheal cells from WT C57BL/6 mice were performed as previously described with minor modifications (54). Briefly, the cells were isolated from bronchial main branches and collected by centrifugation and then suspended in 200 μl/trachea of DNase solution and incubated 5 min on ice, centrifuged at 1,400 rpm for 5 min at 4 °C, and resuspended in 10 ml of F-12K nutrient mixture containing 10% FBS. A 6-well tissue culture plate (Corning) was coated with poly-L-lysine (100 mg/ml, Sciencell) at 37 °C for 1 h followed by thoroughly washing with double distilled water. The cell pellets were suspended with pAECs complete medium which contains DMEM–Ham's F-12 (1:1 v/v), 15 mmol/liter HEPES, 3.6 mmol/liter sodium bicarbonate, 4 mmol/liter L-glutamine, 100 units/ml penicillin, 100 μg/ml streptomycin, 0.25 μg/ml fungizone, 10 μg/ml insulin, 5 μg/ml transferrin, 0.1 μg/ml cholera toxin, 25 ng/ml epidermal growth factor, 30 μg/ml bovine pituitary extract, 10% FBS, and 0.01 mmol/liter retinoic acid (54).

Cell culture in vitro

Cell suspensions were plated into 6-well plates and incubate at 37 °C and 5% CO_2 for 5 h for a negative selection for fibroblasts. Unattached cells were collected, and plates were rinsed twice with 2 ml of pAEC complete medium. Cell suspension and washes were pooled together in a 50-ml conical tube and centrifuged at 1,400 rpm for 5 min. Cell pellets were resuspended with pAECs complete medium and seeded into 6-well tissue culture plate in a concentration of 1×10^5 cells/well at 37 °C and 5% CO_2 for 9 days. Medium was changed on the third day for the first time and was subsequently changed every other day. The cells were enriched to 50–70% for the experiments as described below. The average yield of tracheal cells was 1.2×10^6 cells/trachea obtained from 50 C57BL/6 mice weighing 15–20 g. Cell viability determined by trypan blue exclusion was over 90%. Cytocentrifuge preparations of these cells revealed that over 99% expressed cytokeratin, as determined by pan-cytokeratin antibody staining (results not shown).

Cell stimulation in vitro

To prepare cells for stimulation, pAECs were seeded in a density of 5×10^5 cells/well in a 6-well tissue culture plate (Costar; Corning) and grown until 80% confluence. Next, pAECs were incubated for 6 or 24 h with 500 μg/ml OVA. Cell culture supernatants and cell lysates were collected for detection of protein and mRNA. pAECs were pretreated with10 nmol/liter MCC950 (dissolved in PBS) for 6 h to inhibit NLRP3 (36) or with 10 nmol/liter adapalene (dissolved in PBS) for 6 h to activate RXR$\alpha/\beta/\gamma$, or with 7.5 μmol/liter hemin or 7.5 μmol/liter SnPP for 2 h to induce HO-1 expression or to inhibit its activity or with 25 μmol/liter CO-RM2 (solubilized in DMSO, Sigma–Aldrich) or 50 μmol/liter unconjugated bilirubin (dissolved in 0.1 N NaOH, Sigma–Aldrich) for 4 h, respectively. Partial cells were subsequently treated with 500 μg/ml OVA for

Table 1
Mouse primers

	Forward (5′-3′)	Reverse (5′-3′)
IL-25	CGTCCCACTTTACCACAACC	ACACACACACAAGCCAAGGA
IL-33	AGTCTCCTGCCTCCCTGAGT	CCTGGTCTTGCTCTTGGTCT
TSLP	TGAAAGGGGCTAAGTTCGAG	AAATGTTTTGTCGGGGAGTG
GM-CSF	TGGTCTACAGCCTCTCAGCA	GACGACTTCTACCTCTTCATTCAAC

24 h. For other experiments, pAECs were treated with 10 nmol/liter MCC950 (dissolved in PBS) for 6 h followed by 10 nmol/liter adapalene (dissolved in PBS) for 6 h and were subsequently treated with 500 μg/ml OVA for 24 h for flow cytometry. RXRα siRNA (Santa Cruz Biotechnology, Santa Cruz, CA) was used according to the manufacturer's directions. Preparation of hemin for *in vitro* use was as follows: 1.25 g of hemin was dissolved in 0.1 mol/liter NaOH, diluted with PBS, and titrated to pH 7.5 with 0.2 mol/liter HCl.

The human bronchial epithelial cell line (BEAS-2B) was obtained from American Type Culture Collection. To perform co-IP, BEAS-2B were cultured in DMEM (Gibco) supplemented with 10% heat-inactivated FBS (Gibco), 100 units/ml penicillin (Gibco), and 100 μg/ml streptomycin (Gibco) at 37 °C and 5% CO_2. To induce HO-1 expression, BEAS-2B was also pretreated with 7.5 nmol/liter hemin or with 7.5 nmol/liter hemin and 7.5 nmol/liter SnPP for 2 h, respectively, and subsequently stimulated with 500 μg/ml OVA for 24 h. The cell lysates were collected for detection of protein and subsequent co-IP assay.

ELISA

Analysis of serum OVA-sIgE (Serotec, Kidlington, UK) and other cytokines (IL-4, IL-5, IL-13, TSLP, and CCL2) was performed with ELISA kits (Biolegend, San Diego, CA) as previously described (55).

Flow cytometry

Basophils and DCs in the lung were detected by flow cytometry. Briefly, single cells from lung tissues were first treated with 10 μg/ml anti-FcγRII/III for 30 min at 4 °C followed by treatment with fluorescence-labeled anti-mouse FcϵRIα, c-Kit, and CD49b antibodies in 100 μl of staining buffer (5% FBS in PBS). After being washed twice, the samples were analyzed on a FACSCalibur (BD Bioscience, San Jose, CA). For the detection of apoptosis, pAECs were pretreated with MCC950, adapalene, and hemin as described above, followed by stimulation with 500 μg/ml OVA for 24 h, collected after 24 h, and stained with 5 μl of FITC–annexin V in 150 μl of 1× binding buffer for 15 min. Then the cells were stained with 5 μl of propidium iodide (PI) and detected by flow cytometry to evaluate the number of apoptotic cells as shown by annexin V^+ PI^+ cells. Flow cytometry results were analyzed using FlowJo (StarTree).

Real-time PCR

Total mRNA of pAECs or BEAS-2B was isolated using the RNeasy kit (Qiagen). For reverse transcription, 1 μg of mRNA was used to generate cDNA followed by quantitative PCR using SYBR Green (Qiagen) to assess expression of IL-25, IL-33, TSLP, and GM-CSF. The primers are listed in Table 1. Quantitative PCR using SYBR Green was performed according to the manufacturer's directions.

The preparation and transfection of HO-1 and NLRP3 domain expression plasmids and RXR$\alpha/\beta/\gamma$ subunit expression plasmids

Four NLRP3 domain expression plasmids were constructed including domains of LRR, NACHT, Pyrin, and FISNA based on the conserved domains of NLRP3, and three RXR$\alpha/\beta/\gamma$ subunit expression plasmids were prepared including subunits of RXRα, RXRβ, and RXRγ based on the conserved domains of RXR$\alpha/\beta/\gamma$ on PubMed, respectively. According to previous studies, pCMV-GFP–labeled LRR, NACHT, Pyrin, and FISNA expression plasmids were constructed and named LRR, NACHT, Pyrin, and FISNA, respectively (Shanghai Xitubio Biotechnology Co., Ltd). pcDNA3 HO-1 was constructed in our laboratory. For co-immunoprecipitation assays, HO-1 and pCMV-GFP–labeled NLRP3 domain expression plasmids or HO-1 and pCMV-GFP–labeled RXR$\alpha/\beta/\gamma$ subunit expression plasmids were co-transfected into 293T cells, respectively, using Lipofectamine 2000 as a transfection reagent according to the manufacturer's instructions.

Western blotting

Right lung lobe homogenates, pAECs, or BEAS-2B cells were prepared and solubilized with ice-cold radioimmune precipitation assay buffer (Beyotime) supplemented with protease and phosphatase inhibitor mixture (Thermo Fisher Scientific). Co-IP was performed as described previously (31). Immunoblot analysis was performed, and membranes were blotted with antibodies to RXR$\alpha/\beta/\gamma$, HO-1 (Santa Cruz Biotechnology, Santa Cruz, CA), NLRP3, Bcl-XL, β-actin, β-tubulin, and GAPDH (Cell Signaling Technology, Danvers, MA).

Lung histology and TUNEL assay

The lungs were fixed in 4% formaldehyde overnight and embedded in paraffin. Lung sections of 5 μm were stained with hematoxylin and eosin, periodic acid-Schiff stain (PAS), Masson and evaluated by light microscopy (Olympus, Tokyo, Japan). TUNEL assay kits (Roche) were used to detect cells undergoing apoptosis.

Statistical analysis

For all experiments, we calculated the difference between groups by Student's t test or analysis of variance (GraphPad Prism version 5.0, GraphPad Software). Differences were considered to have significance when $p < 0.05$.

Author contributions—J. L., W. S., C. D., M. W., and Z. X. conceptualization; J. L. and W. S. data curation; J. L. and W. S. formal analysis; J. L., Q. Y., M. Z., X. L., and Z. X. methodology; J. L. and W. S. writing-original draft; W. S. and Z. X. visualization; C. D., M. W., and Z. X. writing-review and editing; Z. X. supervision; Z. X. validation; Z. X. project administration.

Acknowledgments—We thank the staff of Research Center for Experimental Medicine of Ruijin Hospital affiliated with Shanghai Jiao Tong University School of Medicine and flow cytometry core facility at Shanghai Jiao Tong University School of Medicine.

References

1. Lambrecht, B. N., and Hammad, H. (2015) The immunology of asthma. *Nat. Immunol.* **16,** 45–56 CrossRef Medline
2. Tesfaigzi, Y. (2006) Roles of apoptosis in airway epithelia. *Am. J. Respir. Cell Mol. Biol.* **34,** 537–547 CrossRef Medline
3. Thornberry, N. A., and Lazebnik, Y. (1998) Caspases: enemies within. *Science* **281,** 1312–1316 CrossRef Medline
4. Adams, J. M., and Cory, S. (1998) The Bcl-2 protein family: arbiters of cell survival. *Science* **281,** 1322–1326 CrossRef Medline
5. Cryns, V., and Yuan, J. (1998) Proteases to die for. *Genes Dev.* **12,** 1551–1570 CrossRef Medline
6. Tesfaigzi, Y., Fischer, M. J., Daheshia, M., Green, F. H., De Sanctis, G. T., and Wilder, J. A. (2002) Bax is crucial for IFNg-induced resolution of allergen-induced mucous cell metaplasia. *J. Immunol.* **169,** 5919–5925 CrossRef Medline
7. Vignola, A. M., Chanez, P., Campbell, A. M., Souques, F., Lebel, B., Enander, I., and Bousquet, J. (1998) Airway inflammation in mild intermittent and in persistent asthma. *Am. J. Respir. Crit. Care Med.* **157,** 403–409 CrossRef Medline
8. Wadsworth, S. J., Atsuta, R., McIntyre, J. O., Hackett, T. L., Singhera, G. K., and Dorscheid, D. R. (2010) IL-13 and TH2 cytokine exposure triggers matrix metalloproteinase 7–mediated Fas ligand cleavage from bronchial epithelial cells. *J. Allergy Clin. Immunol.* **126,** 366–374 CrossRef Medline
9. Saxon, J. A., Cheng, D. S., Han, W., Polosukhin, V. V., McLoed, A. G., Richmond, B. W., Gleaves, L. A., Tanjore, H., Sherrill, T. P., Barham, W., Yull, F. E., and Blackwell, T. S. (2016) p52 overexpression increases epithelial apoptosis, enhances lung injury, and reduces survival after lipopolysaccharide treatment. *J. Immunol.* **196,** 1891–1899 CrossRef Medline
10. Anderson, O. A., Finkelstein, A., and Shima, D. T. (2013) A2E induces IL-1β production in retinal pigment epithelial cells via the NLRP3 inflammasome. *PLoS One* **8,** e67263 CrossRef Medline
11. Li, Y., Liu, M., Zuo, Z., Liu, J., Yu, X., Guan, Y., Zhan, R., Han, Q., Zhang, J., Zhou, R., Sun, R., Tian, Z., and Zhang, C. (2017) TLR9 regulates the NF-κB–NLRP3–IL-1β pathway negatively in *Salmonella*-induced NKG2D-mediated intestinal inflammation. *J. Immunol.* **199,** 761–773 CrossRef Medline
12. Martinon, F. (2008) Detection of immune danger signals by NALP3. *J. Leukoc. Biol.* **83,** 507–511 CrossRef Medline
13. Kim, R. Y., Pinkerton, J. W., Essilfie, A. T., Robertson, A. A. B., Baines, K. J., Brown, A. C., Mayall, J. R., Ali, M. K., Starkey, M. R., Hansbro, N. G., Hirota, J. A., Wood, L. G., Simpson, J. L., Knight, D. A., Wark, P. A., *et al.* (2017) Role for NLRP3 inflammasome-mediated, IL-1β–dependent responses in severe, steroid-resistant asthma. *Am. J. Respir. Crit. Care Med.* **196,** 283–297 CrossRef Medline
14. Besnard, A. G., Guillou, N., Tschopp, J., Erard, F., Couillin, I., Iwakura, Y., Quesniaux, V., Ryffel, B., and Togbe, D. (2011) NLRP3 inflammasome is required in murine asthma in the absence of aluminum adjuvant. *Allergy* **66,** 1047–1057 CrossRef Medline
15. Schmitz, N., Kurrer, M., and Kopf, M. (2003) The IL-1 receptor 1 is critical for Th2 cell type airway immune responses in a mild but not in a more severe asthma model. *Eur. J. Immunol.* **33,** 991–1000 CrossRef Medline
16. Kadoya, H., Satoh, M., Sasaki, T., Taniguchi, S., Takahashi, M., and Kashihara, N. (2015) Excess aldosterone is a critical danger signal for inflammasome activation in the development of renal fibrosis in mice. *FASEB J.* **29,** 3899–3910 CrossRef Medline
17. Bruder-Nascimento, T., Ferreira, N. S., Zanotto, C. Z., Ramalho, F., Pequeno, I. O., Olivon, V. C., Neves, K. B., Alves-Lopes, R., Campos, E., Silva, C. A., Fazan, R., Carlos, D., Mestriner, F. L., Prado, D., Pereira, F. V., *et al.* (2016) NLRP3 inflammasome mediates aldosterone-induced vascular damage. *Circulation* **134,** 1866–1880 CrossRef Medline
18. Núñez, V., Alameda, D., Rico, D., Mota, R., Gonzalo, P., Cedenilla, M., Fischer, T., Boscá, L., Glass, C. K., Arroyo, A. G., and Ricote, M. (2010) Retinoid X receptor α controls innate inflammatory responses through the up-regulation of chemokine expression. *Proc. Natl. Acad. Sci. U.S.A.* **107,** 10626–10631 CrossRef Medline
19. Shankaranarayanan, P., Rossin, A., Khanwalkar, H., Alvarez, S., Alvarez, R., Jacobson, A., Nebbioso, A., de Lera, A. R., Altucci, L., and Gronemeyer, H. (2009) Growth factor-antagonized rexinoid apoptosis involves permissive PPARg/RXR heterodimers to activate the intrinsic death pathway by NO. *Cancer Cell* **16,** 220–231 CrossRef Medline
20. Grenningloh, R., Gho, A., di Lucia, P., Klaus, M., Bollag, W., Ho, I. C., Sinigaglia, F., and Panina-Bordignon, P. (2006) Cutting edge: inhibition of the retinoid X receptor (RXR) blocks T helper 2 differentiation and prevents allergic lung inflammation. *J. Immunol.* **176,** 5161–5166 CrossRef Medline
21. Tenaud, I., Khammari, A., and Dreno, B. (2007) In vitro modulation of TLR-2, CD1d and IL-10 by adapalene on normal human skin and acne inflammatory lesions. *Exp. Dermatol.* **16,** 500–506 CrossRef Medline
22. Bushue, N., and Wan, Y. J. (2010) Retinoid pathway and cancer therapeutics. *Adv. Drug Deliv. Rev.* **62,** 1285–1298 CrossRef Medline
23. Saito-Hakoda, A., Uruno, A., Yokoyama, A., Shimizu, K., Parvin, R., Kudo, M., Saito-Ito, T., Sato, I., Kogure, N., Suzuki, D., Shimada, H., Yoshikawa, T., Fujiwara, I., Kagechika, H., *et al.* (2015) Effects of RXR agonists on cell proliferation/apoptosis and ACTH secretion/Pomc expression. *PLoS One* **10,** e0141960 CrossRef Medline
24. Gozzelino, R., Jeney, V., and Soares, M. P. (2010) Mechanisms of cell protection by heme oxygenase-1. *Annu. Rev. Pharmacol. Toxicol.* **50,** 323–354 CrossRef Medline
25. Poss, K. D., and Tonegawa, S. (1997) Heme oxygenase 1 is required for mammalian iron reutilization. *Proc. Natl. Acad. Sci. U.S.A.* **94,** 10919–10924 CrossRef Medline
26. Pamplona, A., Ferreira, A., Balla, J., Jeney, V., Balla, G., Epiphanio, S., Chora, A., Rodrigues, C. D., Gregoire, I. P., Cunha-Rodrigues, M., Portugal, S., Soares, M. P., and Mota, M. M. (2007) Heme oxygenase-1 and carbon monoxide suppress the pathogenesis of experimental cerebral malaria. *Nat. Med.* **13,** 703–710 CrossRef Medline
27. Zwerina, J., Tzima, S., Hayer, S., Redlich, K., Hoffmann, O., Hanslik-Schnabel, B., Smolen, J. S., Kollias, G., and Schett, G. (2005) Hemeoxygenase 1 (HO-1) regulates osteoclastogenesis and bone resorption. *FASEB J.* **19,** 2011–2013 CrossRef Medline
28. Chora, A. A., Fontoura, P., Cunha, A., Pais, T. F., Cardoso, S., Ho, P. P., Lee, L. Y., Sobel, R. A., Steinman, L., and Soares, M. P. (2007) Heme oxygenase-1 and carbon monoxide suppress autoimmune neuroinflammation. *J. Clin. Invest.* **117,** 438–447 CrossRef Medline
29. Xia, Z. W., Zhong, W. W., Xu, L. Q., Sun, J. L., Shen, Q. X., Wang, J. G., Shao, J., Li, Y. Z., and Yu, S. C. (2006) Heme oxygenase-1-mediated CD4+CD25 high regulatory T cells suppress allergic airway inflammation. *J. Immunol.* **177,** 5936–5945 CrossRef Medline
30. Bakhautdin, B., Das, D., Mandal, P., Roychowdhury, S., Danner, J., Bush, K., Pollard, K., Kaspar, J. W., Li, W., Salomon, R. G., McMullen, M. R., and Nagy, L. E. (2014) Protective role of HO-1 and carbon monoxide in ethanol-induced cell death in hepatocytes and liver injury in mice. *J. Hepatol.* **61,** 1029–1037 CrossRef Medline
31. Lin, X. L., Lv, J. J., Lv, J., Di, C. X., Zhang, Y. J., Zhou, T., Liu, J. L., and Xia, Z. W. (2017) Heme oxygenase-1 directly binds to STAT3 to control the generation of pathogenic Th17 cells during neutrophilic airway inflammation. *Allergy* **72,** 1972–1987 CrossRef Medline
32. Nakamura, M., Matute-Bello, G., Liles, W. C., Hayashi, S., Kajikawa, O., Lin, S. M., Frevert, C. W., and Martin, T. R. (2004) Differential response of human lung epithelial cells to Fas-induced apoptosis. *Am. J. Pathol.* **164,** 1949–1958 CrossRef Medline
33. Vignola, A. M., Chanez, P., Chiappara, G., Siena, L., Merendino, A., Reina, C., Gagliardo, R., Profita, M., Bousquet, J., and Bonsignore, G. (1999) Evaluation of apoptosis of eosinophils, macrophages, and T lymphocytes in mucosal biopsy specimens of patients with asthma and chronic bronchitis. *J. Allergy Clin. Immunol.* **103,** 563–573 CrossRef Medline
34. Xia, Z. W., Xu, L. Q., Zhong, W. W., Wei, J. J., Li, N. L., Shao, J., Li, Y. Z., Yu, S. C., and Zhang, Z. L. (2007) Heme oxygenase-1 attenuates ovalbumin-

induced airway inflammation by up-regulation of foxp3 T-regulatory cells, interleukin-10, and membrane-bound transforming growth factor-1. *Am J Pathol* **171,** 1904–1914 CrossRef Medline

35. Cao, X., Liu, W., Lin, F., Li, H., Kolluri, S. K., Lin, B., Han, Y. H., Dawson, M. I., and Zhang, X. K. (2004) Retinoid X receptor regulates Nur77/TR3-dependent apoptosis by modulating its nuclear export and mitochondrial targeting. *Mol. Cell. Biol.* **24,** 9705–9725 CrossRef Medline
36. Lin, B., Kolluri, S. K., Lin, F., Liu, W., Han, Y. H., Cao, X., Dawson, M. I., Reed, J. C., and Zhang, X. K. (2004) Conversion of Bcl-2 from protector to killer by interaction with nuclear orphan receptor Nur77/TR3. *Cell* **116,** 527–540 CrossRef Medline
37. Zimmerman, T. L., Thevananther, S., Ghose, R., Burns, A. R., and Karpen, S. J. (2006) Nuclear export of retinoid X receptor alpha in response to interleukin-1β-mediated cell signaling: roles for JNK and SER260. *J. Biol. Chem.* **281,** 15434–15440 CrossRef Medline
38. Henderson, W. R., Jr, Lewis, D. B., Albert, R. K., Zhang, Y., Lamm, W. J., Chiang, G. K., Jones, F., Eriksen, P., Tien, Y. T., Jonas, M., and Chi, E. Y. (1996) The importance of leukotrienes in airway inflammation in a mouse model of asthma. *J. Exp. Med.* **184,** 1483–1494 CrossRef Medline
39. Coll, R. C., Robertson, A. A., Chae, J. J., Higgins, S. C., Muñoz-Planillo, R., Inserra, M. C., Vetter, I., Dungan, L. S., Monks, B. G., Stutz, A., Croker, D. E., Butler, M. S., Haneklaus, M., Sutton, C. E., Núñez, G., *et al.* (2015) A small-molecule inhibitor of the NLRP3 inflammasome for the treatment of inflammatory diseases. *Nat. Med.* **21,** 248–255 CrossRef Medline
40. Yang, S. M., Ka, S. M., Wu, H. L., Yeh, Y. C., Kuo, C. H., Hua, K. F., Shi, G. Y., Hung, Y. J., Hsiao, F. C., Yang, S. S., Shieh, Y. S., Lin, S. H., Wei, C. W., Lee, J. S., Yang, C. Y., *et al.* (2014) Thrombomodulin domain 1 ameliorates diabetic nephropathy in mice via anti-NF-κB/NLRP3 inflammasome-mediated inflammation, enhancement of NRF2 antioxidant activity and inhibition of apoptosis. *Diabetologia* **57,** 424–434 CrossRef Medline
41. Ocker, M., Herold, C., Ganslmayer, M., Hahn, E. G., and Schuppan, D. (2003) The systemic retimoidadapalene inhibits proliferation and induces apoptosis in colorectal cancer cells *in vitro*. *Int. J. Cancer* **107,** 453–459 CrossRef Medline
42. Lambrecht, B. N., and Hammad, H. (2013) Asthma and coagulation. *N. Engl. J. Med.* **369,** 1964–1966 CrossRef Medline
43. Abraham, N. G., and Kappas, A. (2008) Pharmacological and clinical aspects of hemeoxygenase. *Pharmacol. Rev.* **60,** 79–127 CrossRef Medline
44. Wagener, F. A., Eggert, A., Boerman, O. C., Oyen, W. J., Verhofstad, A., Abraham, N. G., Adema, G., van Kooyk, Y., de Witte, T., and Figdor, C. G. (2001) Heme is a potent inducer of inflammation in mice and is counteracted by hemeoxygenase. *Blood* **98,** 1802–1811 CrossRef Medline
45. Jiang, L., Fei, D., Gong, R., Yang, W., Yu, W., Pan, S., Zhao, M., and Zhao, M. (2016) CORM-2 inhibits TXNIP/NLRP3 inflammasome pathway in LPS-induced acute lung injury. *Inflamm. Res.* **65,** 905–915 CrossRef Medline
46. Xiaoyu, H., Si, H., Li, S., Wang, W., Guo, J., Li, Y., Cao, Y., Fu, Y., and Zhang, N. (2017) Induction of heme oxygenas-1 attenuates NLRP3 inflammasome activation in lipopolysaccharide-induced mastitis in mice. *Int. Immunopharmacol.* **52,** 185–190 CrossRef Medline
47. Rushworth, S. A., and MacEwan, D. J. (2008) HO-1 underlies resistance of AML cells to TNF-induced apoptosis. *Blood* **111,** 3793–3801 CrossRef Medline
48. Rushworth, S. A., Bowles, K. M., Raninga, P., and MacEwan, D. J. (2010) NF-κB–inhibited acute myeloid leukemia cells are rescued from apoptosis by heme oxygenase-1 induction. *Cancer Res.* **70,** 2973–2983 CrossRef Medline
49. Koonin, E. V., and Aravind, L. (2000) The NACHT family: a new group of predicted NTPases implicated in apoptosis and MHC transcription activation. *Trends Biochem. Sci.* **25,** 223–224 CrossRef Medline
50. Linhoff, M. W., Harton, J. A., Cressman, D. E., Martin, B. K., and Ting, J. P. (2001) Two distinct domains within CIITA mediate self-association: involvement of the GTP-binding and leucine-rich repeat domains. *Mol. Cell. Biol.* **21,** 3001–3011 CrossRef Medline
51. Decherf, S., Seugnet, I., Becker, N., Demeneix, B. A., and Clerget-Froidevaux, M. S. (2013) Retinoic X receptor subtypes exert differential effects on the regulation of Trh transcription. *Mol. Cell. Endocrinol.* **381,** 115–123 CrossRef Medline
52. Bi, Y., Gong, M., Zhang, X., Zhang, X., Jiang, W., Zhang, Y., Chen, J., Liu, Y., He, T. C., and Li, T. (2010) Pre-activation of retinoid signaling facilitates neuronal differentiation of mesenchymal stem cells. *Dev. Growth Differ.* **52,** 419–431 CrossRef Medline
53. Mridha, A. R., Wree, A., Robertson, A. A. B., Yeh, M. M., Johnson, C. D., Van Rooyen, D. M., Haczeyni, F., Teoh, N. C., Savard, C., Ioannou, G. N., Masters, S. L., Schroder, K., Cooper, M. A., Feldstein, A. E., and Farrell, G. C. (2017) NLRP3 inflammasome blockade reduces liver inflammation and fibrosis in experimental NASH in mice. *J. Hepatol.* **66,** 1037–1046 CrossRef Medline
54. You, Y., Richer, E. J., Huang, T., and Brody, S. L. (2002) Growth and differentiation of mouse tracheal epithelial cells: selection of a proliferative population. *Am. J. Physiol. Lung Cell Mol. Physiol.* **283,** L1315–L1321 CrossRef Medline
55. Yasui, Y., Nakamura, M., Onda, T., Uehara, T., Murata, S., Matsui, N., Fukuishi, N., Akagi, R., Suematsu, M., and Akagi, M. (2007) Heme oxygenase-1 inhibits cytokine production by activated mast cells. *Biochem. Biophys. Res. Commun.* **354,** 485–490 CrossRef Medline